

Article

Effect of Electric Current Heat Treatment on Commercially Pure Titanium Sheets

Chan Hyeok Lee ^{1,2,†}, Seong-Woo Choi ^{1,†}, P. L. Narayana ^{1,3}, Thi Anh Nguyet Nguyen ⁴, Sung-Tae Hong ⁴ ,
Jae H. Kim ^{1,*}, Namhyun Kang ^{2,*}  and Jae-Keun Hong ¹

¹ Advanced Metals Division, Titanium Department, Korea Institute of Materials Science, Changwon 51508, Korea; rchan0955@kims.re.kr (C.H.L.); rhkdgh@kims.re.kr (S.-W.C.); plnarayana@kims.re.kr (P.L.N.); jkhong@kims.re.kr (J.-K.H.)

² Department of Materials Science and Engineering, Pusan National University, Busan 46241, Korea

³ School of Materials Science and Engineering, Gyeongsang National University, Jinju 52828, Korea

⁴ School of Mechanical Engineering, University of Ulsan, Ulsan 44610, Korea; sweetmoona2@gmail.com (T.A.N.N.); sthong@ulsan.ac.kr (S.-T.H.)

* Correspondence: jaehkim@kims.re.kr (J.H.K.); nhkang@pusan.ac.kr (N.K.)

† These authors contributed equally.

Abstract: Rapid electric current heat treatment has been successfully applied to a cold-rolled sheet of commercially pure titanium (CP Ti). The electric current heat treatment was conducted at various temperatures (400, 500, 600 and 700 °C) by altering the current density (A/mm²). The detailed microstructure and texture evolution was studied using electron backscatter and X-ray diffraction analysis. For comparison, conventional heat treatment at 400, 500 and 600 °C were also applied to the cold-rolled sheets. The electrically heat-treated sample showed a much smaller and uniform grain size with a relatively weak texture than the conventionally heat-treated one. As a result, the electrically heat-treated samples exhibited better tensile properties than conventionally heat-treated samples. Furthermore, the electric current treatment produced minimum sheet distortion and good oxidation resistance compared with the conventional heat treatment.

Keywords: CP titanium; electric current heat treatment; microstructure; tensile properties; oxidation



Citation: Lee, C.H.; Choi, S.-W.; Narayana, P.L.; Nguyet Nguyen, T.A.; Hong, S.-T.; Kim, J.H.; Kang, N.; Hong, J.-K. Effect of Electric Current Heat Treatment on Commercially Pure Titanium Sheets. *Metals* **2021**, *11*, 783. <https://doi.org/10.3390/met11050783>

Academic Editor: Maciej Motyka

Received: 9 April 2021

Accepted: 9 May 2021

Published: 11 May 2021

Publisher's Note: MDPI stays neutral with regard to jurisdictional claims in published maps and institutional affiliations.



Copyright: © 2021 by the authors. Licensee MDPI, Basel, Switzerland. This article is an open access article distributed under the terms and conditions of the Creative Commons Attribution (CC BY) license (<https://creativecommons.org/licenses/by/4.0/>).

1. Introduction

Recent years have witnessed significant interest in commercially pure titanium (CP Ti) for power generation, electrochemical and biomedical industries owing to its exceptional corrosion resistance, biocompatibility and high specific strength over other metallic materials [1,2]. However, CP Ti has a critical issue to overcome for structural applications because of its low yield strength. To improve its strength, grain refinement is a commonly used strengthening mechanism based on the Hall–Petch relationship [3–5]. Recently, Chausov et al. [6,7] utilized the complex combined (impact-oscillatory) loading mode to enhance the strength and fracture toughness of Ti-based alloys. In particular, high-reduction cold rolling [8–10], rolling at cryogenic temperatures [3,11] and applying severe plastic deformation with equal channel angular pressing or high-pressure torsion process [12–15] have been adopted for the fabrication of high-strength CP Ti sheets. We previously reported that cold rolling and cryogenic rolling can help the enhancement of the yield strength of CP Ti sheets up to a range of 700–900 MPa under the as-rolled condition, attributed to the formation of a twinning-induced ultrafine-grained microstructure [16,17]. However, owing to the high density of low-angle boundaries and dislocations, severely deformed CP Ti sheets tend to exhibit low ductility and formability.

Applying heat treatment, such as stress relieving and annealing, to deformed materials can effectively improve their microstructure and mechanical properties, particularly ductility and fatigue performance [18,19]. However, conventional heat treatment may deteriorate the material quality and properties mainly because of grain coarsening, surface oxidation

and shape distortion of thin parts [20–22]. Furthermore, heat treatment conducted in a thermal furnace is a time and energy-consuming process. Therefore, an advanced method is required for the heat treatment of severely deformed CP Ti sheets.

In recent years, pulsed electric current treatment, which involves directly applying a high-density electric current to a material, has been suggested as an alternative to conventional heat treatments [23–28]. Especially, the electric current heat treatment got great attention in the sheet metal processing of titanium and magnesium alloys [29,30]. Due to high-density electric current and less electropulsing time, the electric current heat treatment provides effective grain refinement since the recrystallized grains have not enough time to grow [31]. Several researchers have been found the formation of ultrafine-grained microstructure and improved mechanical properties of various alloy systems utilizing the electric heat treatment [29–32]. For instance, Park et al. [25] revealed that electropulsing treatment could accelerate the recrystallization of sheet materials with an athermal effect distinct from Joule heating and effectively reduce the annealing time and temperature. Zhao et al. [27] reported that an electric current-treated Ti-6Al-4V alloy shows improved mechanical properties over the conventionally heat-treated one owing to phase transformation and enhanced texture development.

Thus, considering the severely cold-rolled CP Ti sheets show a remarkably high strength but limited ductility. In the present work, an attempt was made to modify the microstructure and texture by applying an electric current treatment to increase the ductility. Such an improvement in the strength–ductility balance was realized by grain growth restriction and the development of a weak texture. The benefits of electric current treatment in terms of specimen geometry, oxidation resistance, mechanical properties and microstructural analyses are discussed.

2. Experimental Procedure

A hot-rolled and mill-annealed ASTM grade 1 level CP Ti plate with a thickness of 3 mm was obtained from POSCO, Korea, and used as the initial material in this study. The contents of interstitial solutes were 1200, 30, 3 and 6.7 ppm for oxygen, nitrogen, carbon and hydrogen, respectively. The initial CP Ti plate was subjected to cold rolling at room temperature to a final thickness of 0.8 mm with a total reduction of 73.3%. The cold-rolled sheet was subsequently machined with a width of 50 mm and a length of 150 mm and subjected to electric current treatment at 400–700 °C. The electric current treatment was conducted at the University of Ulsan, Korea, and the detailed procedure of the electric current treatment has been described elsewhere [28]. As schematically shown in Figure 1, the titanium sheet was positioned between copper electrodes, and an electric current was applied along the longitudinal direction for 0.5 s. Table 1 lists the experimental parameters related to electric current treatment. For an accurate comparison between the processing temperatures, the current was applied for a constant duration of 0.5 s under all conditions. During electric current treatment and cooling, the temperature history and temperature profile were measured using an infrared thermal imaging camera calibrated with a thermocouple. For comparison, a conventional heat treatment in the range of 400–600 °C was also conducted using a thermal furnace followed by air cooling.

The microstructural features and recrystallization behavior was studied using optical microscopy (OM), (Olympus GX51, Seoul, Republic of Korea) scanning electron microscopy (SEM), (JEOL, Tokyo, Japan) coupled with energy-dispersive X-ray spectroscopy (EDS) and electron backscatter diffraction (EBSD). The crystallographic texture was analyzed using an X-ray diffraction (XRD) instrument obtained from POSTECH, Korea. Five different pole figures, namely (10.0), (00.2), (10.1), (10.2) and (10.3), were measured up to a tilt angle of 70° using the Schultz reflection method. Longitudinal tensile properties were measured using dog-bone-shaped specimens with a gauge length of 25 mm and a width of 6 mm at a strain rate of 10^{-3} s^{-1} (ASTM-E8).

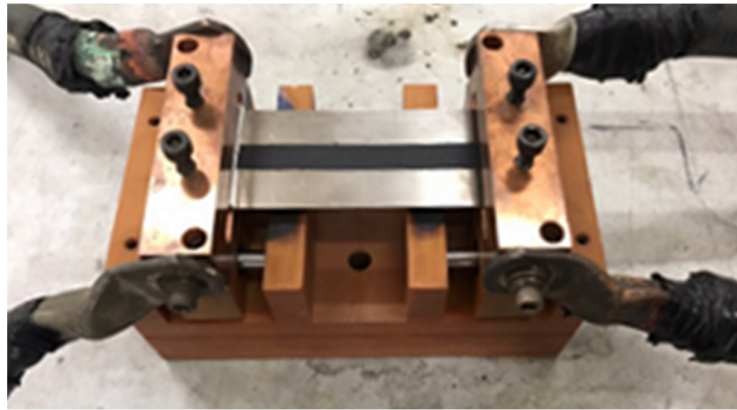


Figure 1. Experimental setup for electric current treatment.

Table 1. List of experimental conditions used for the electric current treatment of CP Ti sheet.

Case	Current density (A/mm ²)	I (kA)	Duration (s)	Temperature (°C)
1	56	2.25	0.5	400
2	60.5	2.42		500
3	66	2.64		600
4	71	2.85		700

3. Results and Discussion

3.1. Electric Current Treatment

When an electric current is applied to a metallic material, heat is generated through the electrical resistance within a relatively short time. For example, at a current density of 66 A/mm², the temperature of the electric current-treated specimen rapidly reaches a peak temperature of 600 °C in 0.5 s and decreases to room temperature in 340 s, as shown in Figure 2. In addition, the image captured using an infrared thermal camera revealed that the temperature was uniformly distributed over the entire sample subjected to peak electric current treatment. Similarly, all the samples were successfully current-treated in the target temperature range of 400–700 °C.

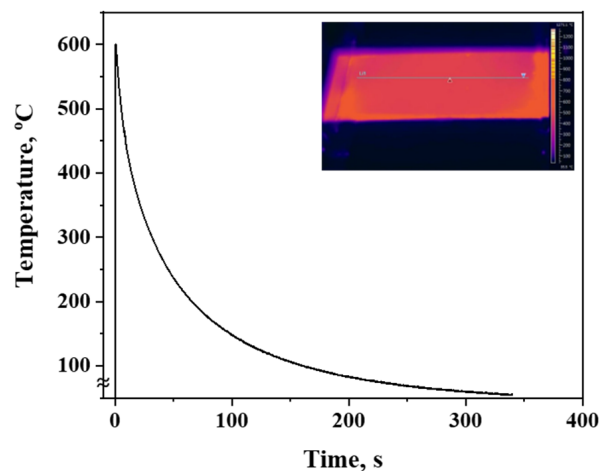


Figure 2. Temperature profile of electric current treated CP Ti with a current density of 66 A/mm². The inset shows the temperature distribution in the sample.

3.2. Microstructure Evolution

Figure 3a shows the EBSD inverse pole figure map of the as cold-rolled CP Ti sheets. Plastic deformation leads to the development of elongated grains along the rolling direction with a relatively low dislocation density and a large number of shear bands with a high dislocation density which could not be identified by EBSD, and it presents as a black area in the inverse pole figure map, as reported in previous works [3]. Choi et al. [16] revealed that the combination of grain orientation, grain size and grain morphology could result in the formation of inhomogeneous microstructures.

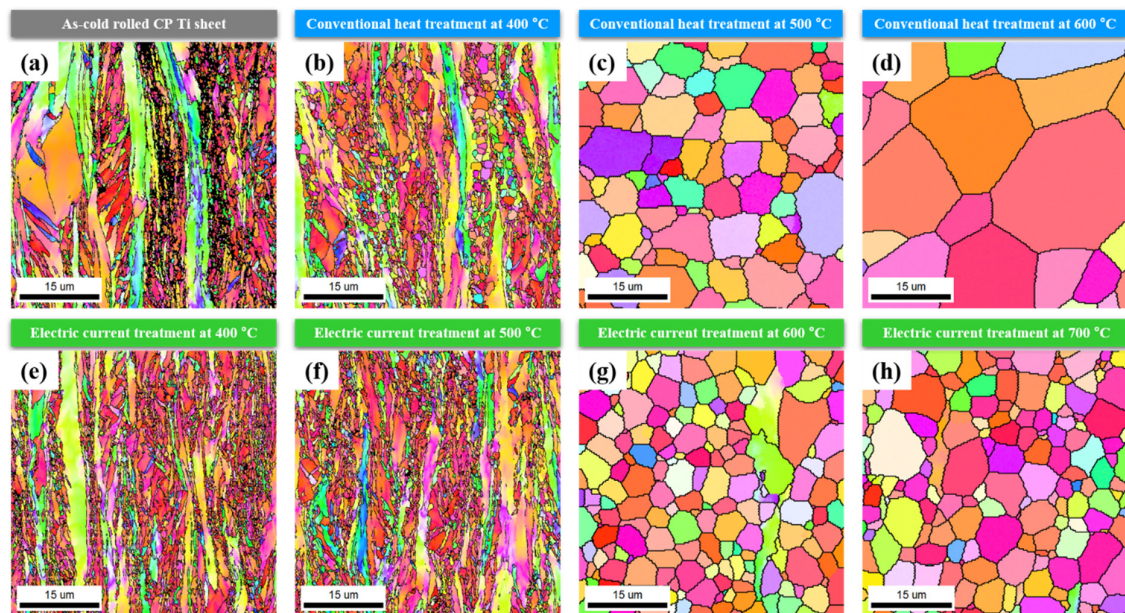


Figure 3. EBSD IPF maps of (a) as-received sample, microstructural evolution during conventional heat treatment (b–d) and electric current treatment (e–h) at various temperatures.

Figure 3b–d show the conventionally heat-treated microstructure of CP Ti sheets treated at 400, 500 and 600 °C for 1 h, respectively. At 400 °C, recrystallization occurred mostly near the shear bands, and a small amount of recrystallized grains could be observed near the elongated grains (Figure 3b). To examine the amount of recrystallization activity, the recrystallized grains were identified based on a grain orientation spread value lower than 1° [33]. The area fraction of the recrystallized region in the sample annealed at 400 °C is 26.3%, with an average grain size of 0.94 μm. After being heat-treated at 500 °C, the sample showed a fully annealed microstructure with an average grain size of 7.2 μm. Upon increase in the heat treatment temperature up to 600 °C, the grains exhibit dramatic coarsening with an average grain size of 17.0 μm.

Figure 3e–g show the electric current-treated microstructure of CP Ti sheets at 400, 500 and 600 °C, respectively. Unlike the conventionally heat-treated specimen, the electric current-treated specimen did not show any recrystallization behavior at 400 °C, as shown in Figure 3e. The electric current treatment at 400 °C applied for a short duration (0.5 s) is insufficient for the activation of recrystallization. At 500 °C, recrystallization begins and the area fraction of the recrystallized region is 19.7%, which is similar to that of the specimen conventionally heat-treated at 400 °C. The average grain size of the recrystallized grains is 0.54 μm. At 600 °C, 84.1% of the area shows recrystallization with an average grain size of 5.0 μm. To obtain a fully annealed microstructure by applying an electric current, an additional treatment was conducted with the peak temperature increased to 700 °C. Interestingly, there was no grain coarsening even at a high processing temperature, and the size of the uniformly recrystallized grains was 5.9 μm.

3.3. Texture Evolution

The texture is also an important factor, particularly for sheet materials. Figure 4 shows the (00.2) pole figures of the alloy sheets under various conditions obtained by XRD. The results show that the texture of the cold-rolled CP Ti sheet (Figure 4a) can be described by a broadened angular distribution of the basal poles from the normal direction toward the transverse direction, as well as by the splitting of the basal poles tilted 30–50° toward the transverse direction, a texture that is typical of rolled α -titanium alloys [17,34]. As shown in Figure 4b, heat treatment at 400 °C did not significantly change the texture. After conventional heat treatment at 500 °C and 600 °C, the splitting of the basal poles in the transverse direction was strengthened with the gradual increase in the maximum intensity as 5.9 and 6.2, respectively (Figure 4c,d).

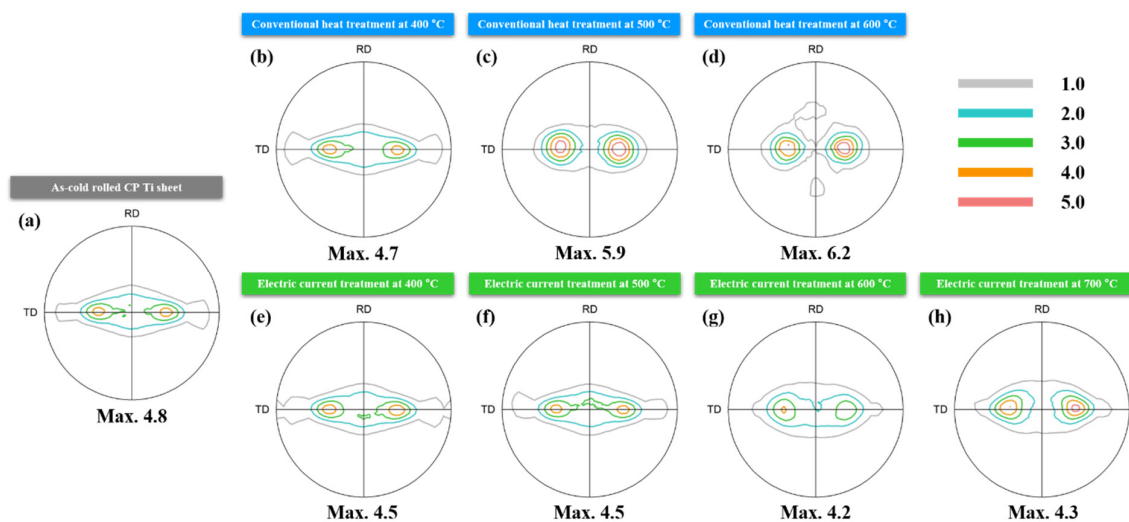


Figure 4. Texture evolution in as-cold rolled CP Ti sheet (a), during conventional heat treatment (b–d) and electric current treatment (e–h).

As shown in Figure 4e–h, the texture evolution, particularly in terms of the angular distribution of the basal poles during electric current treatment, is not significantly different from that observed in the conventionally heat-treated specimen. However, the maximum intensity of the basal pole slightly decreases with an increase in the processing temperature, which is opposite to that observed in the conventional heat treatment.

3.4. Effect of Electric Current Treatment on Recrystallization Behavior

Such a difference between conventional and electric current treatments in terms of the microstructure and texture evolution can be explained by the recrystallization behaviors during post-processing. For a detailed comparison of the early recrystallization behavior between the two cases, the recrystallized grains in the specimen conventionally heat-treated at 400 °C and the electric current-treated sample at 500 °C were selected and the respective microstructure and texture pole figures are shown in Figure 5. Interestingly, the average grain size of the electric current-treated sample (Figure 5c) in the early stages is much smaller than that of the conventionally heat-treated specimen (Figure 5a). The average grain size of electric current and conventional heat treatment specimen was noted as 0.54 μm and 0.94 μm , respectively. In addition, the recrystallized grains in the conventionally heat-treated specimens show texture development in which the basal pole distribution is similar to the as-rolled and overall texture with high intensity.

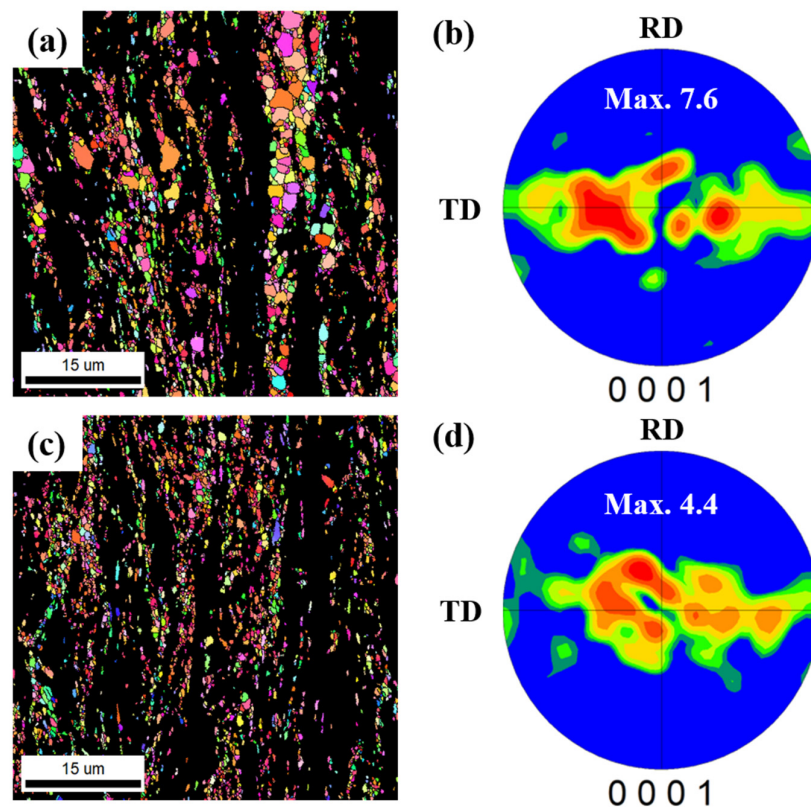


Figure 5. Early-stage recrystallization of a specimen subjected to conventional heat treatment (a,b) and electric current treatment (c,d) and respective texture pole figures.

The recrystallized grains in the conventionally heat-treated specimen can be divided into two groups: ones with a size $\geq 1.1 \mu\text{m}$ and ones with a size $< 1.1 \mu\text{m}$ (Figure 6a). As shown in Figure 6b, smaller grains have relatively weak and randomly distributed orientations, and larger grains tend to show a strengthened texture (Figure 6c). This is mainly due to the different recrystallization mechanisms occurring in each case. In metallic materials, five recrystallization mechanisms have been proposed: (i) grain boundary nucleation [35], (ii) sub-grain boundary migration [36], (iii) particle stimulated nucleation (PSN) [37], (iv) shear band induced nucleation (SBIN) [38–40] and (v) deformation twin induced nucleation (DTIN) [41,42]. In the case of small recrystallized grains, they are found near unidentified regions by the EBSD comprising shear bands and a large number of deformation twins. SBIN and DTIN occur near heavily deformed regions and have a much higher driving force for nucleation and rapid nucleation compared with the other recrystallization mechanisms [38–42]. Kim et al. [33] also reported that SBIN and DTIN exhibit relatively random orientations compared to other recrystallization mechanisms. As a result, small grains can have a weak texture and small size. On the other hand, larger recrystallized grains were observed near the elongated grains. Larger grains are nucleated with sub-grain boundary migration within the elongated grains during heating and have a similar orientation as their parent grains [36]. In addition, larger grains tend to have a similar size as their parent grain width owing to dislocation re-arrangement perpendicular to the elongated direction. As a result, larger grains can have a strong texture with a relatively larger size (Figure 6c). Compared with the heat-treated specimen, the recrystallization mechanism of the electric current treated samples is predominantly SBIN and DTIN because of the short processing time for generating sub-grain boundary migration. Thus, a small grain size is possible with a relatively weak texture, which is an advantage for deformation [17]—such a microstructure and texture evolution during recrystallization affected by further treatment. In addition, the short duration of the

electric current treatment could suppress the grain growth, resulting in a small grain size, whereas the grains in the heat-treated sample were dramatically coarsened with further heat treatment.

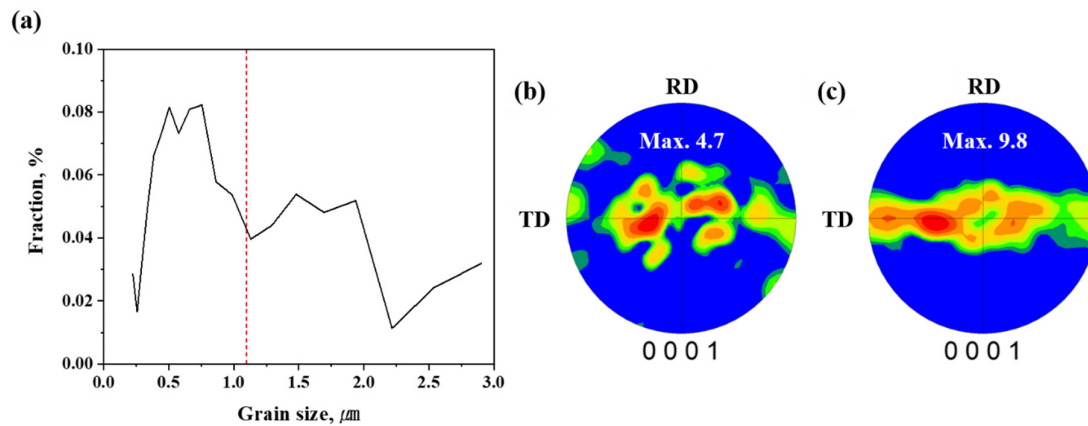


Figure 6. (a) Recrystallized grain size variation in the conventionally heat-treated sample and texture pole figures for (b) smaller grains (<1.1 μm) and (c) larger grains (≥1.1 μm).

3.5. Effect of Electric Current Treatment on Mechanical Properties

Figure 7a shows the tensile properties of the as-cold rolled CP Ti sheet after heat treatment and electric current treatment at various temperatures. In both the treatments, the elongation increased with increasing temperature, whereas the yield strength and ultimate tensile strength decreased. In particular, the mechanical properties dramatically changed after full recrystallization in both cases. However, there were differences in the degree to which the elongation increased and strength degradation with increasing temperature between the heat-treated and current-treated specimens after full recrystallization. In the case of conventional heat treatment, the specimen heat-treated at 500 °C showed the highest elongation (36.8%) and both the strength and elongation decreased after 600 °C, mainly due to grain coarsening and texture strengthening [43]. In comparison, the electric-treated sample exhibited higher strength and elongation than the heat-treated specimen. This is consistent with the microstructure and texture evolution result in that a smaller grain size with a relatively weak texture could enhance the mechanical properties [44,45]. In addition, grain growth is effectively restricted and shows a good strength–elongation combination at higher temperatures. The strength–ductility balance of the materials can be examined using the relationship $YS-EL$ and $I = YS \times EL$ (Figure 7b,c, respectively) [4,16]. For the conventional heat treatment, the maximum value of I was 11.4 GPa at 500 °C. In the case of the electric current treatment, the maximum value of I was 15.4 GPa at 600 °C. This result indicates that the strength–ductility balance was enhanced by the electric current treatment.

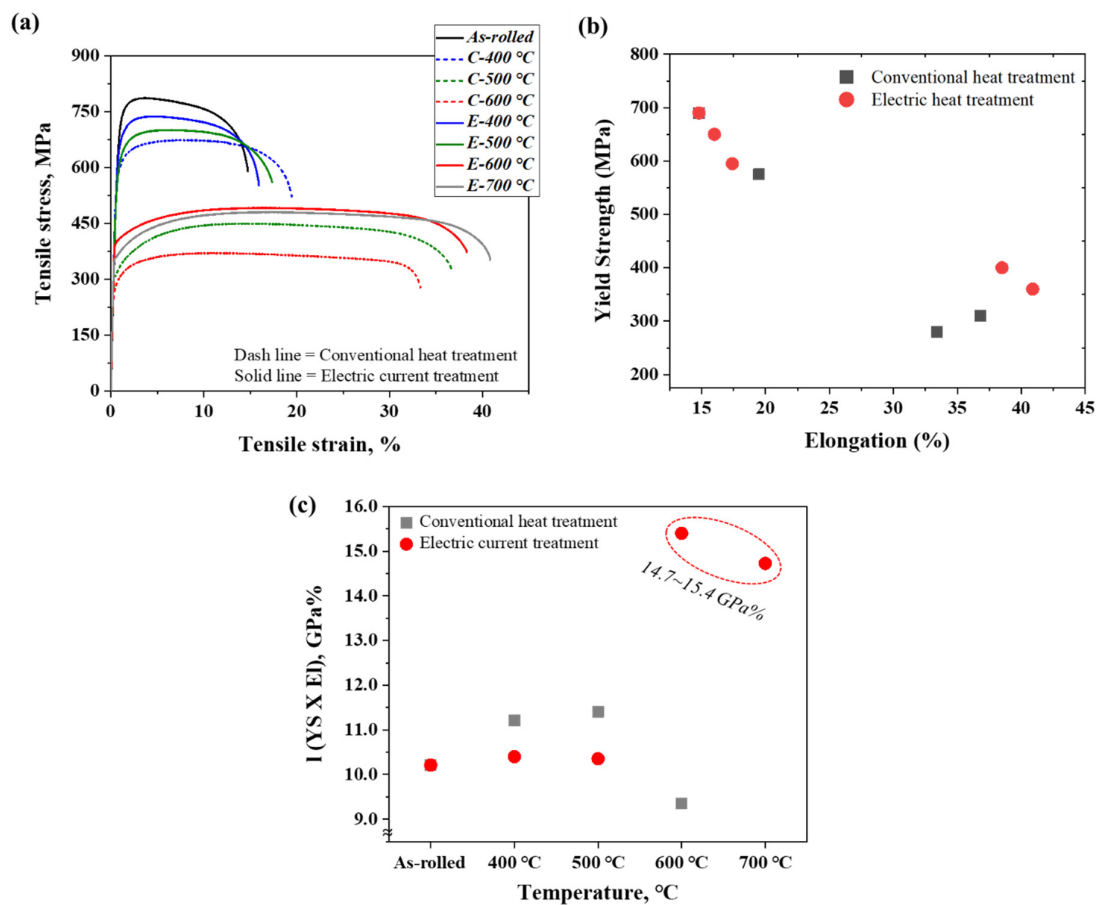


Figure 7. Room-temperature tensile properties of CP Ti processed under various conditions (a), YS-El and YS×El comparison plot of conventionally heat-treated and electric current-treated CP Ti (b,c), respectively, where the red and gray dots indicated the electric current treatment and conventional heat treatment, respectively.

3.6. Effect of Electric Current Treatment on Sheet Shape and Oxidation

As mentioned previously, the electric current treatment is not only an effective method for saving time and improving the mechanical properties but is also beneficial for preventing oxidation and distortion of thin sheets. Figure 8 shows the overall shape of the sheets after applying conventional heat treatment and electric treatment at 600 °C. The conventionally heat-treated sheet is severely bent, and the oxide layer covers the entire surface. In comparison, the electric current-treated specimen shows a relatively flat configuration with a small change in the color on the surface. For a detailed analysis, a cross-section of the specimens was prepared for microstructural observation, as illustrated in Figure 9. Figure 9a,b show the backscattered electron micrographs of the oxide scales of the thermal and electric treated specimens at 600 °C, respectively. A thick layer of oxide scale (8.5 μm) was formed during heat treatment, which loosened the middle layer of the oxide scale, indicating spallation. In contrast, the oxide scale of the electric current-treated sample was thin, compact and adhered to the base alloy owing to the short duration of the treatment. The oxygen distribution analysis results shown with the EDS mapping (Figure 9c,d) also clearly indicate the difference in the oxide behaviors between the two samples. It can be concluded that the electric current-treated sheet has the advantages of short processing time and enhanced mechanical properties, sheet distortion and oxidation resistance. Thus, the electric current heat treatment method provides a lot of possibilities to control and regulate the amount of supplied energy, thereby the microstructure, mechanical properties and corrosion resistance.



Figure 8. Shape changes in CP Ti sheet after applying conventional heat treatment and electric current treatment at 600 °C.

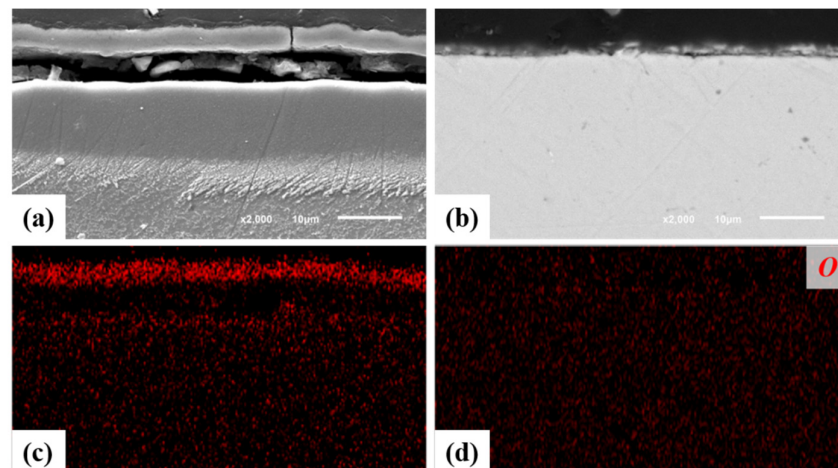


Figure 9. The thickness of the oxide scale and respective oxygen EDS mapping of conventional (a,c) and electric heat-treated (b,d) CP Ti sheets at 600 °C.

4. Conclusions

The present study revealed that the electric current heat treatment has considerable benefits as compared with the conventional heat treatment. From the observed results, the following conclusions are drawn:

- (i) The electric current treatment results in the development of finer microstructure with relatively weak texture as compared to the conventional heat treated sample due to the difference in recrystallization behavior.
- (ii) In the case of electric current heat treatment, the smaller recrystallized grains nucleated near the shear bands and deformation twins with relatively random orientations.

Besides, recrystallization in the conventional heat treatment is occurred by the sub-grain boundary migration within the elongated grains during heating and has a similar orientation as their parent grains with relatively larger grain size.

- (iii) Due to the refined grain morphology with weak texture intensity, the room-temperature tensile properties of the electric current treatment samples were superior to those of the conventional heat-treated specimens.
- (iv) The degree of distortion and the oxidation resistance of electric heat-treated samples was significantly improved as compared with the conventional heat-treated ones due to the rapid processing time.

Author Contributions: Conceptualization, J.H.K., N.K. and J.-K.H.; methodology, T.A.N.N., S.-W.C. and P.L.N.; software, T.A.N.N. and C.H.L.; validation, S.-T.H. and N.K.; formal analysis, J.H.K.; investigation, C.H.L. and J.H.K. resources, J.-K.H.; data curation, S.-W.C. and P.L.N.; writing—original draft preparation, C.H.L. and J.H.K.; writing—review and editing, J.-K.H., S.-T.H. and N.K.; visualization, S.-W.C. and P.L.N.; supervision, N.K. and J.H.K.; project administration, J.-K.H. and S.-T.H.; funding acquisition, J.-K.H. and S.-T.H.; All authors have read and agreed to the published version of the manuscript.

Funding: This work was supported by the Ministry of Trade, Industry and Energy (Grant No. 16-CM-MA-10 and 10077677) and supported by grants from the Fundamental Research Program (Grant No. PNK7520) of the Korea Institute of Materials Science. S.-T. Hong and T. A. Nguyet Nguyen were supported by the National Research Foundation of Korea (NRF) grant funded by the Korean government (MSIT) (No. 2019R1A2C2009939).

Institutional Review Board Statement: Not applicable.

Informed Consent Statement: Not applicable.

Data Availability Statement: The data presented in this study are available on request from the corresponding author.

Acknowledgments: This work was supported by the Ministry of Trade, Industry and Energy (Grant No. 16-CM-MA-10 and 10077677) and supported by grants from the Fundamental Research Program (Grant No. PNK7520) of the Korea Institute of Materials Science. S.-T. Hong and T. A. Nguyet Nguyen were supported by the National Research Foundation of Korea (NRF) grant funded by the Korean government (MSIT) (No. 2019R1A2C2009939).

Conflicts of Interest: The authors declare no conflict of interest.

References

- Gerd, L.; Williams James, C. *Titanium*; Springer: Berlin/Heidelberg, Germany, 2003; pp. 149–175.
- Lütjering, G.; Williams, J.C. Commercially Pure (CP) Titanium and Alpha Alloys. In *Titanium*; Springer: Berlin/Heidelberg, Germany, 2007; pp. 175–201.
- Zherebtsov, S.V.; Dyakonov, G.S.; Salem, A.A.; Sokolenko, V.I.; Salishchev, G.A.; Semiatin, S.L. Formation of nanostructures in commercial-purity titanium via cryorolling. *Acta Mater.* **2013**, *61*, 1167–1178. [[CrossRef](#)]
- Won, J.W.; Lee, J.H.; Jeong, J.S.; Choi, S.W.; Lee, D.J.; Hong, J.K.; Hyun, Y.T. High strength and ductility of pure titanium via twin-structure control using cryogenic deformation. *Mater. Sci. Eng. A* **2020**, *178*, 94–98. [[CrossRef](#)]
- Won, J.W.; Lee, S.; Park, S.H.; Kang, M.; Lim, K.R.; Park, C.H.; Na, Y.S. Ultrafine-grained CoCrFeMnNi high-entropy alloy produced by cryogenic multi-pass caliber rolling. *J. Alloys Compd.* **2018**, *742*, 290–295. [[CrossRef](#)]
- Chausov, M.G.; Maruschak, P.O.; Hutsaylyuk, V.; Sniezek, L.; Pylypenko, A.P. Effect of complex combined loading mode on the fracture toughness of titanium alloys. *Vacuum* **2018**, *147*, 51–57. [[CrossRef](#)]
- Chausov, M.; Maruschak, P.; Pylypenko, A.; Markashova, L. Enhancing plasticity of high-strength titanium alloys VT 22 under impact-oscillatory loading. *Philos. Mag.* **2017**, *97*, 389–399. [[CrossRef](#)]
- Kameyama, T.; Matsunaga, T.; Sato, E.; Kuribayashi, K. Suppression of ambient-temperature creep in CP-Ti by cold-rolling. *Mater. Sci. Eng. A* **2009**, *510–511*, 364–367. [[CrossRef](#)]
- Alkhezraji, H.; Salih, M.Z.; Zhong, Z.; Mhaede, M.; Brokmeier, H.-G.; Wagner, L.; Schell, N. Estimation of Dislocation Density in Cold-Rolled Commercially Pure Titanium by Using Synchrotron Diffraction. *Metall. Mater. Trans. B* **2014**, *45*, 1557–1564. [[CrossRef](#)]
- Kim, W.J.; Yoo, S.J.; Lee, J.B. Microstructure and mechanical properties of pure Ti processed by high-ratio differential speed rolling at room temperature. *Scr. Mater.* **2010**, *62*, 451–454. [[CrossRef](#)]

11. Dyakonov, G.S.; Zharebtsov, S.V.; Klimova, M.V.; Salishchev, G.A. Microstructure evolution of commercial-purity titanium during cryorolling. *Phys. Met. Metallogr.* **2015**, *116*, 182–188. [[CrossRef](#)]
12. Stolyarov, V.V.; Zhu, Y.T.; Alexandrov, I.V.; Lowe, T.C.; Valiev, R.Z. Influence of ECAP routes on the microstructure and properties of pure Ti. *Mater. Sci. Eng. A* **2001**, *299*, 59–67. [[CrossRef](#)]
13. Ko, Y.G.; Shin, D.H.; Park, K.-T.; Lee, C.S. An analysis of the strain hardening behavior of ultra-fine grain pure titanium. *Scr. Mater.* **2006**, *54*, 1785–1789. [[CrossRef](#)]
14. Fattah-alhosseini, A.; Keshavarz, M.K.; Mazaheri, Y.; Reza, A. Strengthening mechanisms of nano-grained commercial pure titanium processed by accumulative roll bonding. *Mater. Sci. Eng. A* **2017**, *693*, 164–169. [[CrossRef](#)]
15. Sergueeva, A.V.; Stolyarov, V.V.; Valiev, R.Z.; Mukherjee, A.K. Advanced mechanical properties of pure titanium with ultrafine grained structure. *Scr. Mater.* **2001**, *45*, 747–752. [[CrossRef](#)]
16. Choi, S.-W.; Li, C.-L.; Won, J.W.; Yeom, J.-T.; Choi, Y.S.; Hong, J.-K. Deformation heterogeneity and its effect on recrystallization behavior in commercially pure titanium: Comparative study on initial microstructures. *Mater. Sci. Eng. A* **2019**, *764*, 138211. [[CrossRef](#)]
17. Won, J.W.; Park, C.H.; Hong, J.; Lee, C.S.; Hong, S.G. Simultaneous Improvement in the Strength and Formability of Commercially Pure Titanium via Twinning-Induced Crystallographic Texture Control. *Sci. Rep.* **2019**, *9*, 2009. [[CrossRef](#)]
18. Hamada, S.; Noguchi, H. Fatigue characteristics of a notched specimen made of commercially pure titanium. *Theor. Appl. Fract. Mech.* **2020**, *109*, 102764. [[CrossRef](#)]
19. Li, X.; Sun, B.-H.; Guan, B.; Jia, Y.-F.; Gong, C.-Y.; Zhang, X.-C.; Tu, S.-T. Elucidating the effect of gradient structure on strengthening mechanisms and fatigue behavior of pure titanium. *Int. J. Fatigue* **2021**, *146*, 106142. [[CrossRef](#)]
20. Catherine, L.; Hamid, D.C.A. The effect of heat treatment on the tensile strength and ductility of pure titanium grade 2. *IOP Conf. Ser. Mater. Sci. Eng.* **2018**, *429*, 012014. [[CrossRef](#)]
21. Hoseini, M.; Pourian, M.H.; Bridier, F.; Vali, H.; Szpunar, J.A.; Bocher, P. Thermal stability and annealing behaviour of ultrafine grained commercially pure titanium. *Mater. Sci. Eng. A* **2012**, *532*, 58–63. [[CrossRef](#)]
22. Shin, K.R.; Ko, Y.G.; Shin, D.H. Effect of electrolyte on surface properties of pure titanium coated by plasma electrolytic oxidation. *J. Alloys Compd.* **2021**, *509*, S478–S481. [[CrossRef](#)]
23. Leopold, K.; Anatoly, B.; Andreas, C.; En, T.C. Effect of Pulsed Electric Current Treatment on the Corrosion and Strength of Reinforcing Steel. *Mater. Sci. Forum* **2012**, *706–709*, 937–944.
24. Roh, J.-H.; Seo, J.-J.; Hong, S.-T.; Kim, M.-J.; Han, H.N.; Roth, J.T. The mechanical behavior of 5052-H32 aluminum alloys under a pulsed electric current. *Int. J. Plast.* **2014**, *58*, 84–99. [[CrossRef](#)]
25. Park, J.-W.; Jeong, H.-J.; Jin, S.-W.; Kim, M.-J.; Lee, K.; Kim, J.J.; Hong, S.-T.; Han, H.N. Effect of electric current on recrystallization kinetics in interstitial free steel and AZ31 magnesium alloy. *Mater. Charact.* **2017**, *133*, 70–76. [[CrossRef](#)]
26. Yang, C.; Lim, J.A.; Ding, Y.F.; Zhang, W.W.; Li, Y.Y.; Fu, Z.Q.; Chan, F.; Lavernia, E.J. Texture evolution and mechanical behavior of commercially pure Ti processed via pulsed electric current treatment. *J. Mater. Sci.* **2016**, *51*, 10608–10619. [[CrossRef](#)]
27. Zhao, Z.; Wang, G.; Zhang, Y.; Wang, Y.; Hou, H. Fast recrystallization and phase transformation in ECAP deformed Ti–6Al–4V alloy induced by pulsed electric current. *J. Alloys Compd.* **2019**, *786*, 733–741. [[CrossRef](#)]
28. Dinh, K.-A.; Hong, S.-T.; Choi, S.-J.; Kim, M.-J.; Kim, H.N. The Effect of Pre-strain and Subsequent Electrically Assisted Annealing on the Mechanical Behaviors of Two Different Aluminum Alloys. *Int. J. Precis. Eng. Manuf.* **2020**, *21*, 2345–2358. [[CrossRef](#)]
29. Konovalov, S.; Komissarova, I.; Ivanov, Y.; Gromov, V.; Kosinov, D. Structural and phase changes under electropulse treatment of fatigue-loaded titanium alloy VT1-0. *J. Mater. Res. Technol.* **2019**, *8*, 1300–1307. [[CrossRef](#)]
30. Wang, Z.J.; Song, H. Effect of high-density electropulsing on microstructure and mechanical properties of cold-rolled TA15 titanium alloy sheet. *J. Alloys Compd.* **2009**, *470*, 522–530. [[CrossRef](#)]
31. Lee, T.; Magargee, J.; Ng, M.K.; Cao, J. Constitutive analysis of electrically-assisted tensile deformation of CP-Ti based on non-uniform thermal expansion, plastic softening and dynamic strain aging. *Int. J. Plast.* **2017**, *94*, 44–56. [[CrossRef](#)]
32. Guan, L.; Tang, G.; Jiang, Y.; Chu, P.K. Texture evolution in cold-rolled AZ31 magnesium alloy during electropulsing treatment. *J. Alloys Compd.* **2009**, *487*, 309–313. [[CrossRef](#)]
33. Kim, J.H.; Suh, B.-C.; Trang, T.T.T.; Hwang, J.H.; Kim, N.J. Orientations of dynamically recrystallized grains nucleated at double twins in Mg–4Zn–1Sn alloy. *Scr. Mater.* **2019**, *170*, 11. [[CrossRef](#)]
34. Bozzolo, N.; Dewobroto, N.; Grosdidier, T.; Wagner, F. Texture evolution during grain growth in recrystallized commercially pure titanium. *Mater. Sci. Eng. A* **2005**, *397*, 346–355. [[CrossRef](#)]
35. Ion, S.E.; Humphreys, F.J.; White, S.H. Dynamic recrystallisation and the development of microstructure during the high temperature deformation of magnesium. *Acta Mater.* **1982**, *30*, 1909–1919. [[CrossRef](#)]
36. Zhu, K.Y.; Chaubet, D.; Bacroix, B.; Brisset, F. A study of recovery and primary recrystallization mechanisms in a Zr–2Hf alloy. *Acta Mater.* **2005**, *53*, 5131–5140. [[CrossRef](#)]
37. Robson, J.D.; Henry, D.T.; Davis, B. Particle effects on recrystallization in magnesium–manganese alloys: Particle-stimulated nucleation. *Acta Mater.* **2009**, *57*, 2739–2747. [[CrossRef](#)]
38. Sandlöbes, S.; Zaeferrer, S.; Schestakow, I.; Yi, S.; Gonzalez-Martinez, R. On the role of non-basal deformation mechanisms for the ductility of Mg and Mg–Y alloys. *Acta Mater.* **2011**, *59*, 429–439. [[CrossRef](#)]
39. Kim, Y.M.; Mendis, C.; Sasaki, T.; Letzig, D.; Pyczak, F.; Hono, K.; Yi, S. Static recrystallization behaviour of cold rolled Mg–Zn–Y alloy and role of solute segregation in microstructure evolution. *Scr. Mater.* **2017**, *136*, 41–45. [[CrossRef](#)]

40. Basu, I.; Al-Samman, T.; Gottstein, G. Shear band-related recrystallization and grain growth in two rolled magnesium-rare earth alloys. *Mater. Sci. Eng. A* **2013**, *579*, 50–56. [[CrossRef](#)]
41. Li, X.; Yang, P.; Wang, L.N.; Meng, L.; Cui, F.E. Orientational analysis of static recrystallization at compression twins in a magnesium alloy AZ31. *Mater. Sci. Eng. A* **2009**, *517*, 160–169. [[CrossRef](#)]
42. Farzadfar, S.A.; Martin, E.; Sanjari, M.; Essadiqi, E.; Yue, S. Texture weakening and static recrystallization in rolled Mg–2.9 Y and Mg–2.9 Zn solid solution alloys. *J. Mater. Sci.* **2012**, *47*, 5488–5500. [[CrossRef](#)]
43. Kim, N.J. Critical Assessment 6: Magnesium sheet alloys: Viable alternatives to steels? *Mater. Sci. Technol.* **2014**, *30*, 1925–1928. [[CrossRef](#)]
44. Agnew, S.R.; Yoo, M.H.; Tome, C.N. Application of texture simulation to understanding mechanical behavior of Mg and solid solution alloys containing Li or Y. *Acta Mater.* **2001**, *49*, 4277–4289. [[CrossRef](#)]
45. Hantzsche, K.; Bohlen, J.; Wendt, J.; Kainer, K.U.; Yi, S.B.; Letzig, D. Effect of rare earth additions on microstructure and texture development of magnesium alloy sheets. *Scr. Mater.* **2010**, *63*, 725–730. [[CrossRef](#)]